ACS OMEGA

http://pubs.acs.org/journal/acsodf
Article

In Vivo Near-Infrared Fluorescence Resonance Energy Transfer (NIR-FRET) Imaging of MMP-2 in ALI/ARDS in LPS-Treated Mice

Nuha Alekhmimi, Qasem Ramadan, Dana Cialla-May, Jürgen Popp, Khaled Al-Kattan, Ali Alhoshani, and Mohammed Zourob*

Cite This: *ACS Omega* 2024, 9, 3609−3615
Read Online

ABSTRACT: Matrix metalloproteinases (MMPs) are zinc-dependent proteinases that are capable of cleavage of extracellular matrix (ECM) proteins and enzymes and play an important role in lung dysfunction. Specifically, MMP-2 is produced in the lung by alveolar epithelial and endothelial cells and other immune cells, such as macrophages. MMP-2 regulatory pathway is initiated in alveolar macrophages during acute lung injury (ALI), which may increase pulmonary inflammation. Therefore, there is a critical need for fast and reliable techniques to track the acute respiratory distress syndrome (ARDS). Here, we describe near-infrared fluorescence resonance energy transfer (NIR-FRET) MMP-2-based probe for the *in vivo* detection of ALI induced by lipopolysaccharides (LPS). LPS-induced MMP-2 was measured using near-infrared (NIR) imaging after 1, 2, 4, 5, and 24 h of LPS exposure. Our results were compared with the data obtained from ELISA and Western blotting, demonstrating that MMP-2 fluorescence probe provide a promising *in vivo* diagnostic tool for ALI/ARDS in infected mice.

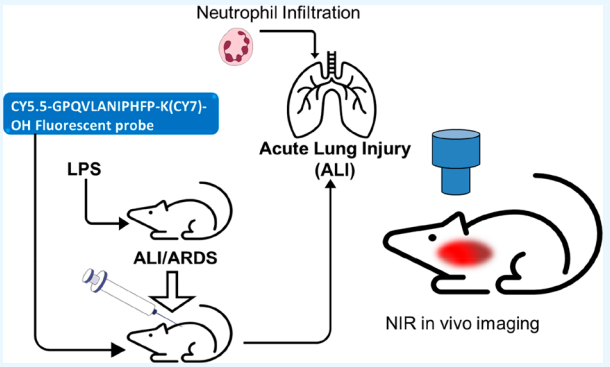

1. INTRODUCTION

Acute lung injury (ALI) and acute respiratory distress syndrome (ARDS) are associated with high rates of mortality and morbidity worldwide. Pathologically, ALI is characterized by an innate immune (inflammatory) response that can develop into a major clinical syndrome, such as ARDS. Common pathophysiologic features of ALI/ARDS are pulmonary leukocyte infiltration, interstitial edema, and impaired gas exchange. Clinically, pulmonary dysfunction is largely attributed to collateral damage induced by the invasion of polymorphonuclear leukocytes (PMN).[1,2] PMN's migration from the pulmonary vasculature and infiltration into the lung alveoli are dependent on the establishment of an alveolar-to-vascular chemotactic gradient.[2,3] Both alveolar epithelial cells and macrophages respond to lung injury and infection by releasing cytokines and chemokines that can initiate the inflammatory response, such as keratinocyte chemoattractant (KC), also known as chemokine (C-X-C motif or CXCL). CXCL1 is a small peptide that belongs to the CXC chemokine family. It is expressed by macrophages, neutrophils, and epithelial cells.[1,3] Furthermore, alveolar macrophages (AMϕ), with their arsenal of inflammatory mediators, are believed to be pivotal effector cells in ALI/ARDS.[3] ARDS is currently diagnosed using imaging techniques, such as chest X-ray and computed tomography (CT) scanning, and laboratory blood tests, which includes an arterial blood gas analysis, complete blood count (CBC), coagulation profile, and measurement of inflammatory markers. The severity of ARDS is determined using the Berlin definition, which proposes three distinct classifications of ARDS based on the degree of hypoxemia: mild (200 mmHg < PaO 2/FiO 2 ≤ 300 mmHg), moderate (100 mmHg < PaO 2/FiO 2 ≤ 200 mmHg), and severe (PaO 2/FiO 2 ≤ 100 mmHg).

The current routine methods for detecting lung injury have proven to be reliable in identifying early signs. However, their effectiveness is limited when it comes to detecting subtle changes in lung function at early stage injury. Consequently, these methods may not be efficient for early detection. Moreover, these methods are time-consuming and necessitate the use of centralized medical laboratories, which can be very costly. These factors further limit their viability as practical and accessible tools for early detection. Therefore, it is crucial to explore alternative approaches that can address the limitations of current methods and offer a more efficient and cost-effective solution for the early detection of lung injury.

Received: October 1, 2023
Revised: December 12, 2023
Accepted: December 14, 2023
Published: January 11, 2024

https://doi.org/10.1021/acsomega.3c07614
ACS Omega 2024, 9, 3609−3615

Matrix metalloproteinases (MMPs), a family of 25 released and cell-surface-bound neutral proteinases,[4] are zinc-dependent proteinases[5−8] that are involved in the degradation of structural components of the extracellular matrix (ECM) and are upregulated in various diseases.[4] MMPs play a major role in lung organogenesis[9,10] and are actively present in a variety of inflammatory disorders, including lung immune disorders and even cancer.[1] However, in a healthy state, not all MMPs exist within the lung tissue—many are upregulated during acute and chronic inflammatory disorders, such as MMP-2.[11] MMP-2 targets all structural proteins in the ECM, cell adhesion molecules, growth factors, cytokines, and chemokines.[12] Due to its multiplicity and complexity, the role of MMP-2 proteolysis in modulating the function of these substrates *in vivo* is not yet fully understood.[13−15] Among the different enzymes secreted by neutrophils, which represent hallmarks of ALI at sites of inflammation, MMP-2 is notable for its pleiotropic effects. MMP-2 has been associated with a wide range of pathological conditions such as cystic fibrosis, emphysema, ALI, sepsis, and heart dysfunction.[5,16,17,17−21] Particularly, MMP-2 plays an important role in inflammatory associated ALI, which might developed to a greater degree due to the remodeling of the ECM.[16] MMP-2 is hence implicated in serious pulmonary pathological conditions.[5,17] Regardless, many studies have implicated MMPs in the lung injury process,[16−18] the role of specific proteases at different phases of injury is currently not fully understood. Therefore, the activity of MMPs in lung injury has gained significant attention through many experimental studies.[7,9,18,19]

Lipopolysaccharides (LPS) are known to induce MMP-2 activation by upregulation of TNF-α in patients' blood and are correlated with sepsis severity. Wang et al.[18] described an electrochemical peptide cleavage-based biosensor for MMP-2 detection with exonuclease-III-assisted cycling signal amplification. They detected 0.15 pg/mL MMP-2 with a dynamic range 0.5 pg/mL to 50 ng/mL. In a previous study, we described a paper-based biosensor for the rapid detection of ALI/ARDS that employed functionalized magnetic nanobeads immobilized on a gold substrate.[19] In the presence of MMPs, the golden surface of the substrate is masked by the beads (i.e., it appears black). Upon the protease's cleavage, the beads are cleared/washed away, and the golden substrate is partially exposed. This change in appearance allows for the simple visual detection of MMP activity. The developed sensor achieved a limit of detection of 5×10^{-4} mg/mL. Despite the abundance of related literature on this matter, it is worth noting that there is still a lack of comprehensive studies that have determined the precise role of MMP-2 in the development and progression of ALI and ARDS. More sophisticated models and techniques are required to enable fast, reliable, and accurate detection of the involved biomarkers. In addition, manipulation of MMP-2 activity in experimental lung injury would enable the collection of mechanistic information rather than phenotypic information on the disease pathogenesis.[19]

In this study, we explored the potential of near-infrared fluorescence (NIRF) imaging as a non-invasive method to assess and detect ARDS. To achieve this, we utilized the specific peptide MMP-2, with the sequence CY5.5-GPQVLANIPHFP-K(CY7)-OH, as a probe for NIRF imaging. We induced lung injury in mice by administering intranasal lipopolysaccharide (LPS), which mimics the conditions of ALI and ARDS. By combining the use of the MMP-2 peptide and NIRF imaging with the LPS-induced lung injury model, our goal was to evaluate the potential of this technique for diagnosing and monitoring ARDS *in vivo*[14] (Scheme 1). The

Scheme 1. NIR-Based Fluorescence Imaging for Assessment and Detection of ARDS using MMP-2 Fluorescence Probes *In Vivo*

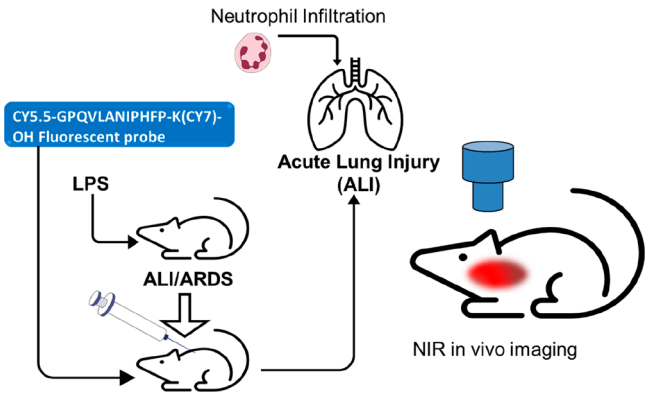

commercial MMP-2 source is known for its reliability and purity, which ensures meeting the necessary standards for accurate imaging. This source is more cost-effective and offers the convenience of bulk quantities in a variety of formats, including frozen protein, concentrated protein, and lyophilized powder and, hence, enables lower cost experimentations. In addition, the commercial source is compatible with a wide range of imaging techniques, including immunohistochemistry, immunofluorescence, and Western blots, therefore enabling the utilization of various analytical and visualizing methods. This biocompatible, optically quenched fluorescence probe generates a strong NIRF signal after enzyme activation[20,21] (e.g., by ALI/ARDS proteases). This approach involves the modification of imaging techniques to enable the accurate and fast detection of the upregulated ARDS marker expression *in vivo* during acute lung permeability.

2. RESULTS AND DISCUSSION

2.1. The LPS-Induced ALI Model. In this study, a newly developed MMP-2-specific protease substrate was used to detect and quantify MMP-2 activity *in vivo* and non-invasively track ALI/ARDS in a mouse model. The sequence used to construct the imaging probe (CY5.5-GPQVLANIPHFP-K-(CY7)-OH) was chosen to be rapidly and selectively cleaved by MMP-2, as MMP-2 enzymes are abundant serine proteases with potentially overlapping substrates.[21,22] LPS was used to induce the ALI in mice. The lung tissues of the ALI mice were harvested within 24 h of LPS treatment. LPS treatment leads to severe pulmonary edema, which is characterized by an increased wet/dry ratio in the lung (data not shown). This observation was further validated by the increase in the level of protein secretions in the bronchoalveolar lavage fluid (BALF) for the LPS-treated mice. Figure 1A−E presents the LPS-induced PMN and AMϕ infiltration into the lung tissue of the mouse. The total neutrophil density in the BALF of the LPS-treated mice was found to be significantly higher (Figure 1B,D) in comparison with the untreated mice (Figure 1A). Figure 1E reveals the migration of neutrophils from the endothelium to the interstitium in response to LPS treatment. Figure 1F displays the PMN and AMϕ counts in tissues with and without LPS treatment. While no PMNs were observed in the untreated group, a significant number of PMNs was

https://doi.org/10.1021/acsomega.3c07614
ACS Omega 2024, 9, 3609−3615

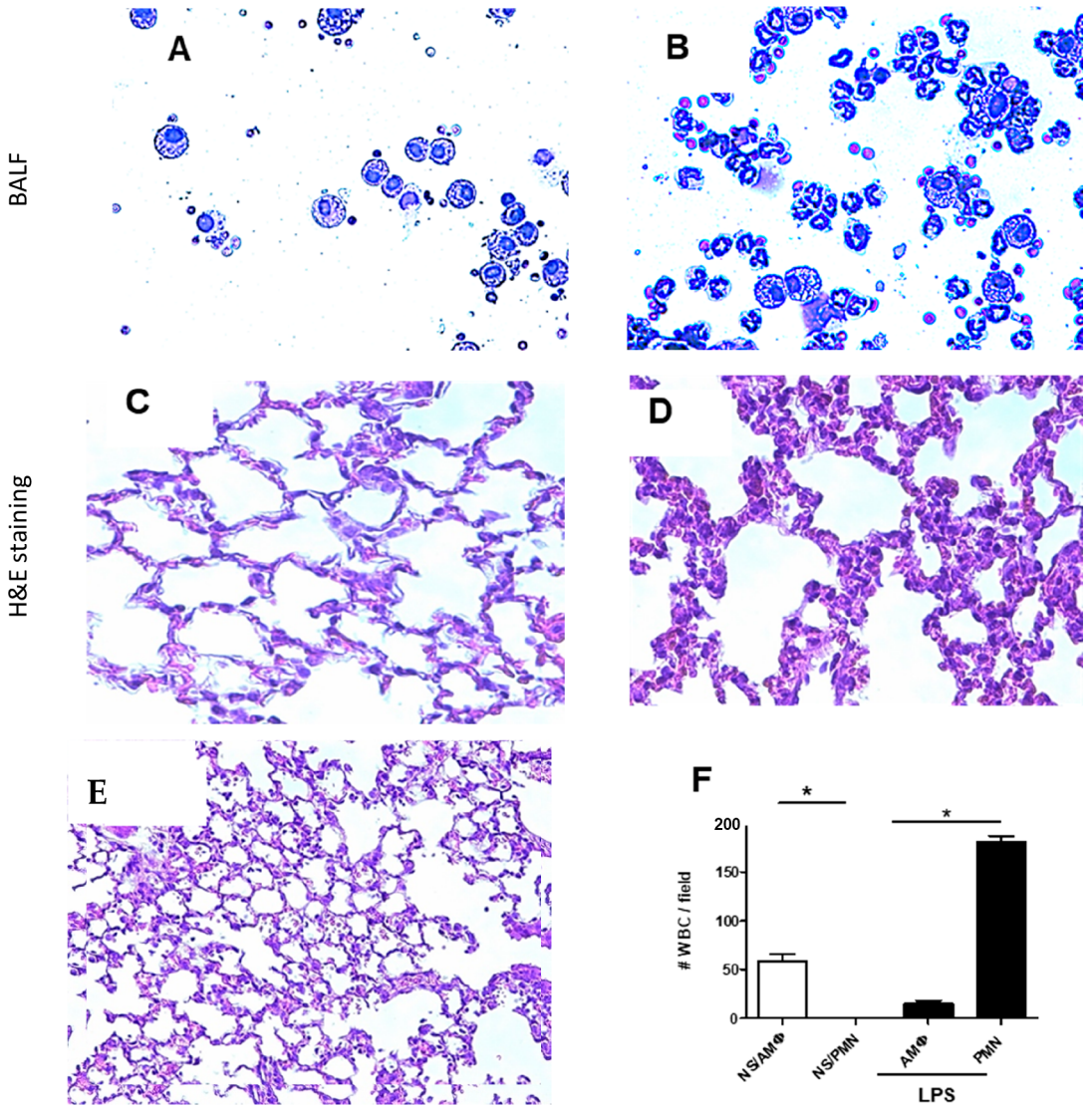

Figure 1. Effect of intranasal LPS on PMN and AMϕ in BALF: (A) BALF obtained from WT mice treated with 50 μL of normal saline (control; Diff-Quick staining was used to visualize and differentiate the cells). (B) BALF collected from WT mice challenged with 50 μg LPS post 4 h administrations. (C) H&E staining in lung tissue of mice treated with normal slain lung tissue. (D) H&E staining in lung tissue of mice treated with LPS lung tissue at 40× magnification. (E) H&E staining in lung tissue of mice treated with LPS lung tissue at 20× magnification. (F) Quantitative data of cell count differentiation, 40× magnification, $n = 3$, $^*P < 0.0001$, control = normal saline (NS).

observed after LPS treatment. In contrast, a notable reduction in the number of AMϕ was observed after LPS treatment. In the LPS-induced mice, 95% of the cells were neutrophils, as determined by the cell count and hematoxylin and eosin (H&E) staining. The concentrations of MMP-2 and KC in the BALF were also significantly elevated in the LPS-treated mice (Figure 2).

2.2. MMP-2 Detection Using ELISA. MMP-2 secretion in BALF was also assessed using enzyme-linked immunosorbent assay (ELISA) and Western blotting. As expected, MMP-2 was significantly elevated in the BALF of LPS-treated mice in comparison with the control group (Figure 2A). Moreover, it was observed that the secretion of MMP-2 was time-dependent. A noticeable increase in MMP-2 expression was observed over the entire duration of the experiment. While there were only slight variations between the 30 min and 2 h challenged groups, a significant magnitude of secretion was observed after 4 and 24 h (Figure 2B). Figure 2C shows a significant increase in KC in the mice treated with the corticosteroid-containing solution compared with the control group treated with normal saline (NS). The elevation of KC, which normally increases in the inflammatory state, indicates the induction of ALI in the mice.

2.3. *In Vivo* Detection of MMP-2 Using NIR-FRET Imaging. Figures 3 and 4 were obtained with near-infrared fluorescence resonance energy transfer (NIR-FRET) imaging, which qualitatively examined the status of the inflammation due to the LPS/MMP-2 treatment. These results are consistent with those obtained from the ELISA and Western blot data (Figure 2). The highest MMP-2 expression was observed after 24 h of LPS treatment. This elevation in the MMP-2 could be attributed to the upregulation of interleukin-33 (IL-33) in LPS-induced ALI mice and LPS-treated mice.[23] It was found that IL-33 induces the expression of MMP-2 and MMP-9 in a STAT3-dependent manner. Therefore, deactivating the IL-33/STAT3/MMP-2/9 pathway[23] could be exploited as a therapeutic strategy for ALI/ARDS. These results reveal that

https://doi.org/10.1021/acsomega.3c07614
ACS Omega 2024, 9, 3609−3615

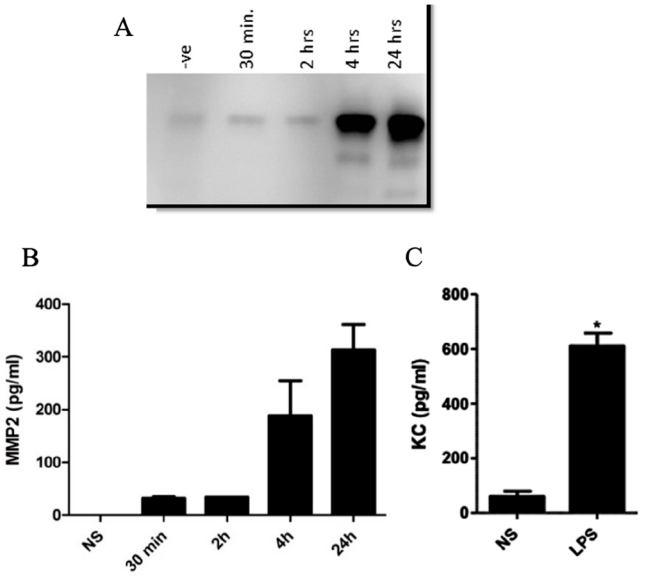

Figure 2. (A) Significant increase of MMP-2 in the BALF of the LPS-treated mice after 4 and 24 h. (B) MMP-2 levels in mice was measured using ELISA after 30 min, 2, 4, and 24 h of LPS treatment. Similarly, MMP-2 secretion was elevated after 4 and 24 h. (C) KC level with/without LPS treatment, NS; control $*P < 0.05$; compared to untreated in the same group; $n = 3$.

MMP-2 is a prominent biomarker that can be employed in identifying ALI/ARDS.

The MMP-2 probe was more rapidly and selectively activated by intranasal LPS application *in vivo*. Fluorescence signals were easily detected in the lung region of the inflamed and control healthy mice (Figure 3). A comparison was made between the MMP-2 activity in the ALI/ARDS mice and that in the control mice that received normal slaine using MMP-2 fluorescent substrate peptide. For example, at 4 h (Figure 3F), lung dysfunction was observed by the MMP-2 probe. MMP-2 cleavage was observed to be significantly high after 5 h of LPS challenge (Figure 3H). This indicated the progression of (right) RT and (left) LT lung damage, which represents the experimental acute lung injury. Collectively, these results demonstrate the capability of NIR to detect LPS-induced ALI/ARDS in mice.

To interpret the obtained imaging results, the ImageJ software was employed by applying a significant threshold of 35% of the averaged mean fluorescence of the LPS-induced mice. The total fluorescence was significantly higher in mice with ALI ($n = 30$; median concentration of 750 nM) in comparison with the healthy controls ($n = 30$; 0 nM), as shown in Figure 4.

The NIR imaging technique offers a highly precise and sensitive approach for detecting and quantifying MMP-2 levels in tissues. This innovative method surpasses traditional techniques by providing a greater depth of penetration into the tissue, allowing for the detection of MMP-2 proteins at a more sensitive and precise level, even when they are present in lower concentrations. Its ability to accurately measure MMP-2 levels, combined with its minimally invasive nature, makes it an invaluable tool in the field of medical imaging. NIR imaging holds significant importance in the study of ALI and ARDS, as demonstrated in this study in mice. One significant advantage is its ability to provide real-time, minimally invasive monitoring of key molecular events associated with ALI/ARDS pathogenesis in live mice. This technique allows for the precise measurement of signaling events *in vivo*, which can help identify potential targets for intervention and assess the efficacy of therapeutic interventions. One limitation is that it may not be able to capture the complex interplay of multiple factors contributing to ALI/ARDS comprehensively.

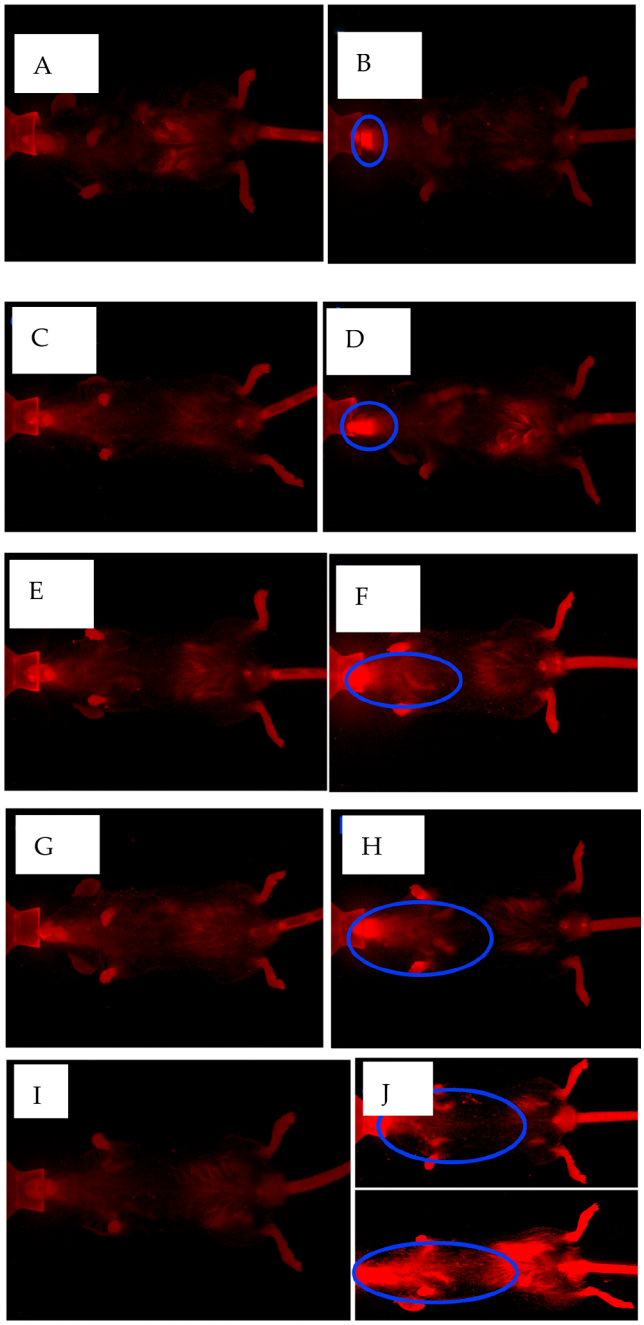

Figure 3. *In vivo* NIR-FRET images obtained from the lung region after inducing ALI in the animals by LPS intranasal administration at different time intervals. (A, C, E, G, I) WT mice treated with 50 μL of normal saline (NS) and the MMP-2 fluorescence probe (control). Images of mice (B) 1, (D) 2, (F) 4, (H) 5, and (J) 24 h after treatment with LPS/MMP-2 fluorescence probe to track intrapulmonary dysfunction, $n = 3$.

3. MATERIALS AND METHODS

3.1. Materials. The MMP-2 near-infrared FRET peptide CY5.5-GPQVLANIPHFP-K(CY7)-OH was synthesized with a

https://doi.org/10.1021/acsomega.3c07614
ACS Omega 2024, 9, 3609−3615

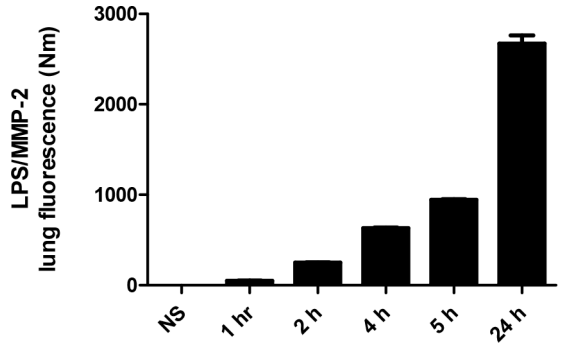

Figure 4. Secretion level of LPS-induced MMP-2 obtained using NIR imaging at 1, 2, 4, 5, and 24 h after LPS challenge. Images were analyzed using ImageJ software.

purity of 98.4% by metabion International (Plangg, Germany). LPS *Escherichia coli* stereotype (026:B6), ethylenediaminetetraacetic acid (EDTA) were purchased from Sigm-Aldrich (St. Louis, Missouri). MMP-2 and KC were obtained from R&D Systems, Germany. The monoclonal mouse E-tag antibody and anti-MMP-2 mouse polyclonal antibody were purchased from ThermoFisher Scientific (Waltham, Massachusetts), and H&E staining was purchased from Abcam (Waltham, Massachusetts).

3.2. Experimental Methods. *3.2.1. Mice.* The study was conducted at the King Saud University (KSU) Animal Facility. Male, 6−10 week old, co-housed, wild-type (WT) mice with a C57BL/6NTac background were obtained from Jackson Laboratory (Bar Harbor, Maine). All mice were kept under standard laboratory conditions with 12 h light/dark cycles and at a temperature of 21 ± 1 °C, and they had free access to food and water. All procedures adopted in this study were conducted in compliance with the Animal Care and Use Committee (ACUC) and the Office of Research Affairs of the Institutional Review Board IRB approved by King Fahad Medical City (NO: FWA00018774).

3.2.2. LPS/MMP-2-Induced Lung Inflammation/Injury. The mice were anesthetized, then the lung inflammation/injury in the mice was induced by intranasal administration of 25 μg of LPS/MMP-2 mixed with 25 μg of fluorescent peptide substrate in 50 μL of normal saline, as previously described, but with minor modification by adding the MMP-2 probe.[19] Five 10 μL drops of the LPS/MMP-2 mixture was applied to the nose. The animals were allowed to recover from anesthesia after LPS treatment. After 4 h, the mice were anesthetized again to obtain bronchoalveolar lavage fluid (BALF). As a control, BALF was also collected from the untreated mice.

3.2.3. BALF Collection. BALF was collected from the WT animal lungs as previously described but with minor modifications.[20] Briefly, a small incision was made in the neck region, and tissue was removed to expose the trachea. The trachea was then cannulated using a 1 cm^3 syringe fitted with a 24G catheter (BD, Utah). The lung was gently infused with 0.6 mL of 37 °C phosphate-buffered saline (PBS) containing 0.2% ethylenediaminetetraacetic acid (EDTA), and this mixture was aspirated back into the syringe. The lungs were washed eight times, and the collected BALF was centrifuged, aliquoted, and stored at −80 °C for later use.

3.2.4. In Vivo Animal Imaging. In vivo imaging experiments were conducted by using the Pearl Impulse small imaging system (LI-COR GmbH, Germany), which enables NIRF detection. The mice were anesthetized with isoflurane gas and then positioned horizontally and exposed directly to the micro-X-ray Pearl Impulse. The MMP-2 dye was successfully detected within the animal body using the NIRF detection mode at a specific wavelength of 680 nm. This detection mode utilizes near-infrared light, allowing for the direct and accurate visualization of the MMP-2 peptide susbtrate conjugated with NIR dye. Illumination due to MMP-2 indicated lung inflammation/injury in the mice. Imaging was performed on the lungs of treated mice induced with LPS at 1, 2, 4, 5, and 24 h after LPS/MMP-2 treatment to track the modulation effect of intrapulmonary MMP-2/LPS administration. Measurements of lung density enabled the detection of ALI/ARDS probes by NIR imaging, which was quantified using ImageJ software.

3.2.5. MMP-2 and KC Measurements by Enzyme-Linked Immunosorbent Assay (ELISA). The mice were treated with LPS, then 1 mL of BALF was collected and centrifuged at 1200 rpm for 5 min at 25 °C. The BALF supernatants were separated and stored at −80 °C in cryovials until analysis. ELISA was performed using protease detection kits to measure the concentrations of MMP-2 and KC. The assay was conducted according to the manufacturer's instructions. Sample absorbance was obtained using ELISA plate reader (R&D Systems, Germany) at 450 nm. Calibration curves for MMP-2 were plotted using data from prior experiments within the range of 30−350 pg/mL. All samples were thawed only once and assayed in triplicate.

3.2.6. Immunoblot Analysis. BALF was collected from the LPS-challenged mice and centrifuged, then equal amounts of total protein were used for each immunoprecipitation, and volumes were adjusted accordingly using elution buffer. Two micrograms of anti-E tag antibodies were added to the lysates with 30 μL of 50% protein A-sepharose suspension. BALF samples were then analyzed by Western blotting. The samples were boiled in a 2× Laemmli sample buffer for separation using sodium dodecyl-sulfate polyacrylamide gel electrophoresis (SDS-PAGE). Proteins were transferred to polyvinylidene difluoride (PVDF) membranes (Immobilon-P, Millipore) for Western blot analysis. The membranes with the appropriate primary antibody were stored overnight at 4 °C. The membranes were washed and probed with horseradish peroxidase (HRP)-linked secondary antibody for 1 h at room temperature and visualized using enhanced chemiluminescence (ECL).

3.2.7. Hematoxylin and Eosin (H&E) Staining. The WT animal group was exposed to LPS for 4 h. The lung lobes were rapidly excised individually and injected with 1 mL of formalin. Subsequently, histological H&E staining was performed on 4 μm sections that were fixed in 10% neutral buffered formalin (NBF), embedded in paraffin, and sectioned and stained with H&E.

3.2.8. Statistical Analysis. *T*-Test was used to compare the two means of healthy and treated samples. An analysis of variance (ANOVA) test (San Diego, California) was used for multiple comparisons, followed by a *t*-test with Bonferroni corrections in GraphPad (San Diego, California, U.S.A.).

4. CONCLUSIONS

We explored the potential of near-infrared fluorescence resonance energy transfer (NIR-FRET) imaging to detect ARDS. In this study, the MMP-2 sensitive fluorescent cleavable peptide substrate was examined in a non-invasive fashion for detection of the MMP-2 activity in a murine model of ALI. The results indicate that the activated MMP-2 acts as a

https://doi.org/10.1021/acsomega.3c07614
ACS Omega 2024, 9, 3609−3615

biomarker for ALI/ARDS. LPS-induced MMP-2 was measured using near-infrared (NIR) imaging after 1, 2, 4, 5, and 24 h of LPS exposure. Furthermore, the quantification of MMP-2 released by the LPS treatment were compared with Western blots and ELISA. NIR-FRET imaging enables safe imaging diagnoses and opens the door to many applications of MMP-2 biosensors to diagnose lung inflammation.

AUTHOR INFORMATION

Corresponding Author

Mohammed Zourob − *Alfaisal University, Riyadh 11533, Saudi Arabia;* orcid.org/0000-0003-2187-1430; Email: mzourob@alfaisal.edu

Authors

Nuha Alekhmimi − *Alfaisal University, Riyadh 11533, Saudi Arabia; Institute of Physical Chemistry (IPC) and Abbe Center of Photonics (ACP), Friedrich Schiller University Jena, Member of the Leibniz Center for Photonics in Infection Research (LPI), 07743 Jena, Germany*

Qasem Ramadan − *Alfaisal University, Riyadh 11533, Saudi Arabia*

Dana Cialla-May − *Institute of Physical Chemistry (IPC) and Abbe Center of Photonics (ACP), Friedrich Schiller University Jena, Member of the Leibniz Center for Photonics in Infection Research (LPI), 07743 Jena, Germany; Leibniz Institute of Photonic Technology, Member of Leibniz Health Technologies, Member of the Leibniz Center for Photonics in Infection Research (LPI), 07745 Jena, Germany*

Jürgen Popp − *Institute of Physical Chemistry (IPC) and Abbe Center of Photonics (ACP), Friedrich Schiller University Jena, Member of the Leibniz Center for Photonics in Infection Research (LPI), 07743 Jena, Germany; Leibniz Institute of Photonic Technology, Member of Leibniz Health Technologies, Member of the Leibniz Center for Photonics in Infection Research (LPI), 07745 Jena, Germany;* orcid.org/0000-0003-4257-593X

Khaled Al-Kattan − *Alfaisal University, Riyadh 11533, Saudi Arabia*

Ali Alhoshani − *Department of Pharmacology and Toxicology, College of Pharmacy, King Saud University, Riyadh 11454, Saudi Arabia;* orcid.org/0000-0002-3450-283X

Complete contact information is available at: https://pubs.acs.org/10.1021/acsomega.3c07614

Notes

The authors declare no competing financial interest.

ACKNOWLEDGMENTS

The authors would like to thank Dr. Yasser A. Alshawakir and the team at the Animal Facility as well as KSU for their technical assistance with the *in vivo* experiments. This research project was funded by Alfaisal University.

REFERENCES

(1) Force, A. D. T.; Ranieri, V.; Rubenfeld, G.; Thompson, B.; Ferguson, N.; Caldwell, E.; Fan, E.; Camporota, L.; Slutsky, A. Acute respiratory distress syndrome: the Berlin Definition. *JAMA* **2012**, *307* (23), 2526−2533.

(2) Kangelaris, K. N.; Prakash, A.; Liu, K. D.; Aouizerat, B.; Woodruff, P. G.; Erle, D. J.; Rogers, A.; Seeley, E. J.; Chu, J.; Liu, T.; Osterberg-Deiss, T.; Zhuo, H.; Matthay, M. A.; Calfee, C. S. Increased expression of neutrophil-related genes in patients with early sepsis-induced ARDS. *American Journal of Physiology-Lung Cellular and Molecular Physiology* **2015**, *308* (11), L1102−L1113.

(3) Daubeuf, F.; Frossard, N. Performing bronchoalveolar lavage in the mouse. *Current protocols in mouse biology* **2012**, *2* (2), 167−175.

(4) Greenlee, K. J.; Werb, Z.; Kheradmand, F. Matrix metalloproteinases in lung: multiple, multifarious, and multifaceted. *Physiol. Rev.* **2007**, *87* (1), 69−98.

(5) Corbel, M.; Boichot, E.; Lagente, V. Role of gelatinases MMP-2 and MMP-9 in tissue remodeling following acute lung injury. *Braz. J. Med. Biol. Res.* **2000**, *33*, 749−754.

(6) Avlonitis, N.; Debunne, M.; Aslam, T.; McDonald, N.; Haslett, C.; Dhaliwal, K.; Bradley, M. Highly specific, multi-branched fluorescent reporters for analysis of human neutrophil elastase. *Organic & biomolecular chemistry* **2013**, *11* (26), 4414−4418.

(7) Xu, F.; Hu, Y.; Zhou, J.; Wang, X. Mesenchymal stem cells in acute lung injury: are they ready for translational medicine? *Journal of cellular and molecular medicine* **2013**, *17* (8), 927−935.

(8) Chu, K.-E.; Fong, Y.; Wang, D.; Chen, C. F.; Yeh, D. Y.-W. Pretreatment of a matrix metalloproteases inhibitor and aprotinin attenuated the development of acute pancreatitis-induced lung injury in rat model. *Immunobiology* **2018**, *223* (1), 64−72.

(9) Winkler, M. K.; Foldes, J. K.; Bunn, R. C.; Fowlkes, J. L. Implications for matrix metalloproteinases as modulators of pediatric lung disease. *American Journal of Physiology-Lung Cellular and Molecular Physiology* **2003**, *284* (4), L557−L565.

(10) Alekhmimi, N. K.; Cialla-May, D.; Ramadan, Q.; Eissa, S.; Popp, J.; Al-Kattan, K.; Zourob, M. Biosensing Platform for the Detection of Biomarkers for ALI/ARDS in Bronchoalveolar Lavage Fluid of LPS Mice Model. *Biosensors* **2023**, *13*, 676.

(11) Buckley, S.; Warburton, D. Dynamics of metalloproteinase-2 and-9, TGF-β, and uPA activities during normoxic vs. hyperoxic alveolarization. *American Journal of Physiology-Lung Cellular and Molecular Physiology* **2002**, *283* (4), L747−L754.

(12) Ries, C.; Egea, V.; Karow, M.; Kolb, H.; Jochum, M.; Neth, P. MMP-2, MT1-MMP, and TIMP-2 are essential for the invasive capacity of human mesenchymal stem cells: differential regulation by inflammatory cytokines. *Blood* **2007**, *109* (9), 4055−4063.

(13) Löffek, S.; Schilling, O.; Franzke, C. Series 'matrix metalloproteinases in lung health and disease'edited by J. Müller-Quernheim and O. Eickelberg number 1 in this series: Biological role of matrix metalloproteinases: A critical balance. *Eur. Respir. J.* **2011**, *38* (1), 191−208.

(14) Johansson, N.; Ahonen, M. Matrix metalloproteinases in tumor invasion. *Cellular and Molecular Life Sciences CMLS* **2000**, *57* (1), 5−15.

(15) Kessenbrock, K.; Plaks, V.; Werb, Z. Matrix metalloproteinases: regulators of the tumor microenvironment. *Cell* **2010**, *141* (1), 52−67.

(16) Petanidis, S.; Kioseoglou, E.; Salifoglou, A. Metallodrugs in targeted cancer therapeutics: aiming at chemoresistance-related patterns and immunosuppressive tumor networks. *Curr. Med. Chem.* **2019**, *26* (4), 607−623.

(17) Nagase, H.; Woessner, J. F. Matrix metalloproteinases. *J. Biol. Chem.* **1999**, *274* (31), 21491−21494.

(18) Wang, D.; Yuan, Y.; Zheng, Y.; Chai, Y.; Yuan, R. An electrochemical peptide cleavage-based biosensor for matrix metalloproteinase-2 detection with exonuclease III-assisted cycling signal amplification. *Chem. Commun.* **2016**, *52* (35), 5943−5945.

(19) Alekhmimi, N.; Popp, J.; Cialla, D.; Zourob, M. Development multiplexing sensing platform for the detection of ALI/ARDS in mice. *Eur. Respiratory Journal* **2019**, *54*, PA802.

(20) Weissleder, R.; Tung, C.-H.; Mahmood, U.; Bogdanov, A. In vivo imaging of tumors with protease-activated near-infrared fluorescent probes. *Nature biotechnology* **1999**, *17* (4), 375−378.

(21) Funovics, M.; Weissleder, R.; Tung, C.-H. Protease sensors for bioimaging. *Anal. Bioanal. Chem.* **2003**, *377* (6), 956−963.

(22) Szarka, R. J.; Wang, N.; Gordon, L.; Nation, P.; Smith, R. H. A murine model of pulmonary damage induced by lipopolysaccharide

via intranasal instillation. *Journal of immunological methods* **1997**, *202* (1), 49−57.
(23) Liang, Y.; Yang, N.; Pan, G.; Jin, B.; Wang, S.; Ji, W. Elevated IL-33 promotes expression of MMP2 and MMP9 via activating STAT3 in alveolar macrophages during LPS-induced acute lung injury. *Cellular & Molecular Biology Letters* **2018**, *23* (1), 52.

https://doi.org/10.1021/acsomega.3c07614
ACS Omega 2024, 9, 3609−3615